

# The challenge of large and empty voids in SDSS DR7 redshift survey

Saeed Tavasoli<sup>1</sup>, Kaveh Vasei<sup>1</sup> and Roya Mohayaee<sup>2</sup>

<sup>1</sup> *Institute for Research in Fundamental Sciences (IPM), P.O. Box 19395-5531, Tehran, Iran*

<sup>2</sup> *Institut d'Astrophysique de Paris (IAP), CNRS, UPMC, 98 bis boulevard Arago, France*

10 October 2012

## ABSTRACT

We produce catalogues of voids for SDSS DR7 redshift survey and for a Millennium I simulation mock data. The mock catalog is constructed such that it closely represents SDSS DR7 survey. We carry a parallel analysis of the two catalogues and find that in both the observation and the simulation, voids tend to be equally spherical. The total volume occupied by the voids and their total number are slightly larger in the simulation than in the observation. We find that large voids are less abundant in the simulation and the total luminosity of the galaxies contained in a void with a given radius is on average higher than observed by SDSS DR7 survey. We expect these discrepancies to be, in fact, even more important than found here since the present value of  $\sigma_8$  given by WMAP7 is lower than the value of 0.9 used in the Millennium I simulation. The reason why the simulation fails to produce enough of the large and dark voids could be due to the failure of certain semi-analytic models of galaxy formation in reducing the small-scale power of  $\Lambda$ CDM and in producing sufficient power on large scales.

**Key words:** cosmology: theory, void, large-scale structure

## 1 INTRODUCTION

Redshift surveys have been demonstrating for a few decades that galaxies are distributed on a cosmic web of filaments, walls and clumps. These structures which form on a hierarchy of scales and span a large redshift range bound regions of low luminosities that are mostly devoid of observable galaxies. These “void” regions occupy more than %80 of the volume of the observable Universe. Since the discovery of voids using Zwicky clusters (Einasto et.al. 1980) and the discovery of the first giant or supervoid in Bootes constellation (Kirshner et al. 1981) numerous works have followed (Zeldovich et al. 1982; Davis et al. 1982; de Lapparent et al. 1986; da Costa et al. 1988; Geller & Huchra 1989; da Costa et al. 1994) and diverse algorithms for void identification have been developed and applied to larger and more complete surveys (see e.g. Vogeley et al. (1991); Neyrinck (2008)).

The formation and evolution of voids is well-understood in the framework of gravitational instability (Zeldovich et al. 1982; Shandarin & Zeldovich 1989). However, when comparing void properties between observations and simulations based on  $\Lambda$ CDM certain problems still remain to be better understood. By definition, voids are devoid of galaxies or contain negligible number of faint galaxies. The perplexing issue is that we do not see a large population of low-mass galaxies populating voids (Klypin et.al. (1999); Moore et.al. (1999)) and furthermore the void galaxies that we see are basically representative of the general population (Peebles 2001).

Observed voids seem to contain fewer galaxies and in particular dwarf galaxies contrary to what is expected from  $\Lambda$ CDM

(Peebles 2001; Tully et al. 2008; Tikhonov & Klypin 2009) Some studies have also shown that voids in observations are significantly larger than those in simulations (Ryden & Turner 1984). Although modifying models of galaxy formation might solve these problems and various remedies such as proper biasing and halo occupation distribution have been proposed (Hoyle et al. 2005; Tinker et al. 2008), different studies suggest that the problem would still persist (Bothun et al. 1986; Little & Weinberg 1994; Plionis & Basilakos 2002; Gottlöber et al. 2003; Hoyle & Vogeley 2004; Goldberg et al. 2005; Hoefl et al. 2006).

The problem of empty and large voids could be due to  $\Lambda$ CDM having too much power on small scales and hence to the problem of over-abundance of substructures (Tikhonov & Klypin 2009). Substructures would occupy the voids making them less empty and statistically they could break larger voids into smaller ones. On the other hand, one could equally infer that  $\Lambda$ CDM lacks power on large scales, perhaps due to the fact that the value of  $\sigma_8$  is too low.

In this work, we study this problem by analysing voids in the SDSS DR7 data and also by carrying a parallel and comparative analysis on a mock SDSS DR7 catalog based on the Millennium I simulation. Our void-finder algorithm is an improved and generalized version of the original algorithm proposed by Aikio & Mae-hoenen (1998). The important feature of this algorithm is that it does not assume a priori that voids are spherical and hence can be used to study the shapes of the voids. We apply our void-finder algorithm to the Sloan Digital Sky Survey SDSS DR7 and build a catalog of voids. In parallel, we also apply our algorithm to a mock SDSS DR7 catalog which we construct out of the Millennium I

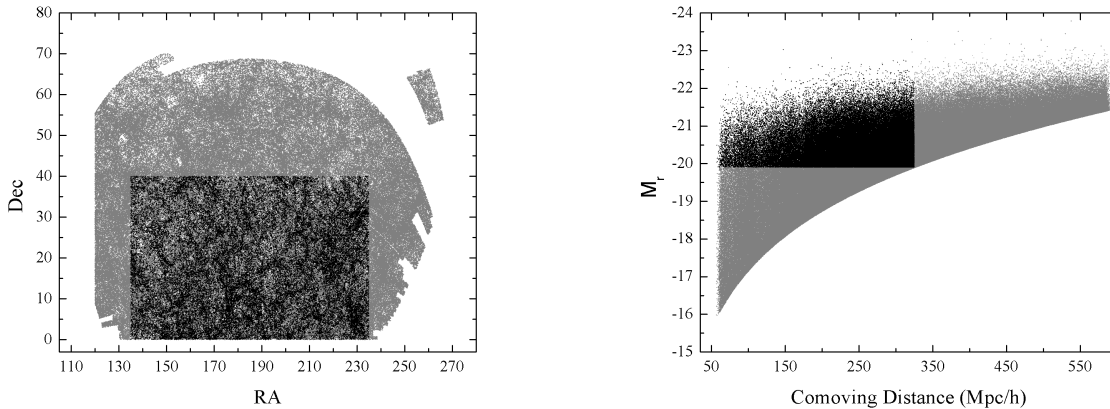


**Figure 1.** Darker shaded areas in both panels show the SDSS DR7 region (left) and the Volume-limited sample (right) that we have selected for this work.

simulation. The mock catalog is given the same magnitude cut-off as SDSS DR7 and in a different version, we also make a mock catalog which has the same number density as SDSS but a different magnitude cut-off. This allows us to compare various properties of observed voids to those predicted by  $\Lambda$ CDM and the semi-analytic model of galaxy formation.

In Section 2, we present our sample, made out of SDSS DR7 catalog. In Section 3, we present our mock catalog. In Section 4, we explain our void-finder algorithm. In Section 5, we find the voids in the simulation and observation catalogues and discuss the numbers, sizes and shapes of the voids. In Section 6, we study the abundance of large voids in the observations and the mock catalogues. In Section 7, luminosities of voids as a function of their sizes are presented and compared between the simulation and the observation. In Section 8, we conclude.

## 2 THE SDSS DR7: DEFINITION OF THE SAMPLE

We have selected the main galaxy sample of the 7th data release of the Sloan Digital Sky Survey (SDSS DR7) (Abazajian et al. 2009). The redshifts of the galaxies are corrected for the motion of the local group and are given in the CMB rest frame. The  $k$ -corrections for the SDSS galaxies are calculated using the KCORRECT algorithm developed by Blanton et al. (2003a) and Blanton & Roweis (2007). The boundaries of our selected region of SDSS is:  $135 < \text{RA} < 235$  and  $0 < \text{DEC} < 40$  which contains 283076 galaxies. All of the objects in this selected region have redshift error smaller than  $2.5 \times 10^{-4}$  and the errors in their apparent “Petrosian” magnitudes of  $r$ -band,  $m_r$ , are smaller than 0.1. The absolute magnitudes of galaxies are determined in the  $r$ -band using cosmological parameters;  $H_0 = 100$  and the density parameters  $\Omega_m = 0.25$  and  $\Omega_\Lambda = 0.75$ . Galaxies belonging to voids are identified by using a volume-limited sample taken from the selected region. The final subsample contains 68702 galaxies with absolute magnitudes  $M_r < -19.9$  which lie in the comoving distance interval 75-325  $h^{-1}$ Mpc, corresponding to  $0.02 < z < 0.12$ .

The selected region of the SDSS DR7 is shown in the left panel of Fig. 1. The right panel of this figure shows the plot of the absolute  $r$ -band magnitude versus comoving distance. The dark region in this plot illustrates the selected volume-limited sample which is used in this work.

## 3 MOCK MILLENNIUM I CATALOG: DEFINITION OF THE SAMPLE

The millennium I simulation is run with  $N = 2160^3$  particles in a comoving box of length  $L = 500h^{-1}$ Mpc with a mass resolution of  $8.6 \times 10^8 h^{-1} M_\odot$ . The adopted cosmology is a  $\Lambda$ CDM model with  $\Omega_m = 0.25$ ,  $\Omega_b = 0.045$ ,  $\Omega_\Lambda = 0.75$ ,  $h = 0.73$ ,  $n = 1$  and  $\sigma_8 = 0.9$ . This value of  $\sigma_8$  is larger than its present value of 0.8 given by WMAP7 (Komatsu et al. 2011), hence yielding more power on larger scales. The evolution of baryons within these dark matter halos is predicted by different semi-analytic models. Current semi-analytic models try to incorporate various complex processes such as gas cooling, reionization, star formation, supernova feedback, metal evolution, black hole growth and AGN feedback (e.g. Bower et al. (2006), De Lucia & Blaizot (2007), Guo et al. (2011)). Although the semi-analytic models are designed to match the observational data as closely as possible, they can still fail in certain aspects, for example the low-mass galaxies with stellar-mass ( $< 10^9 M_\odot$ ) are slightly over-predicted. Consequently to remedy this problem, supernova feedback, a modified law for star formation, or a different cosmological model are evoked (see e.g. Guo et al. (2011); Bower et al. (2012); Wang et al. (2012); Menci et al. (2012)).

In this work, we use the mock galaxy redshift catalog of Blaizot-ALLSky-PT-1<sup>1</sup> which was designed to mimic the SDSS and has an almost identical redshift distribution and a very similar color distribution. This mock catalog was constructed by Blaizot et al. (2005) using the Mock Map Facility (MoMaF) code and the semi-analytic model presented in De Lucia & Blaizot (2007). Furthermore, In order to have a mock catalog that resembles SDSS DR7 galaxy survey as closely as possible, we select a region in the simulation that lies in the same redshift range ( $0.02 < z < 0.12$ ) and has the same geometry. Our mock volume-limited sample includes 68701 galaxies with stellar mass larger than  $10^9 M_\odot$  and brighter than  $M_r < -20.16$ , roughly representing the galaxies brighter than  $M_r < -19.9$  in the SDSS DR7 sample and covering a volume of  $1.2 \times 10^7 (\text{Mpc}/h)^3$  in the volume-limited SDSS DR7. Consequently, the simulation sample has the same galaxy number density as the SDSS DR7 sample.

<sup>1</sup> <http://www.gvo.org/Millennium/Help?page=databases/mpamocks/blaziot2006.allsky>

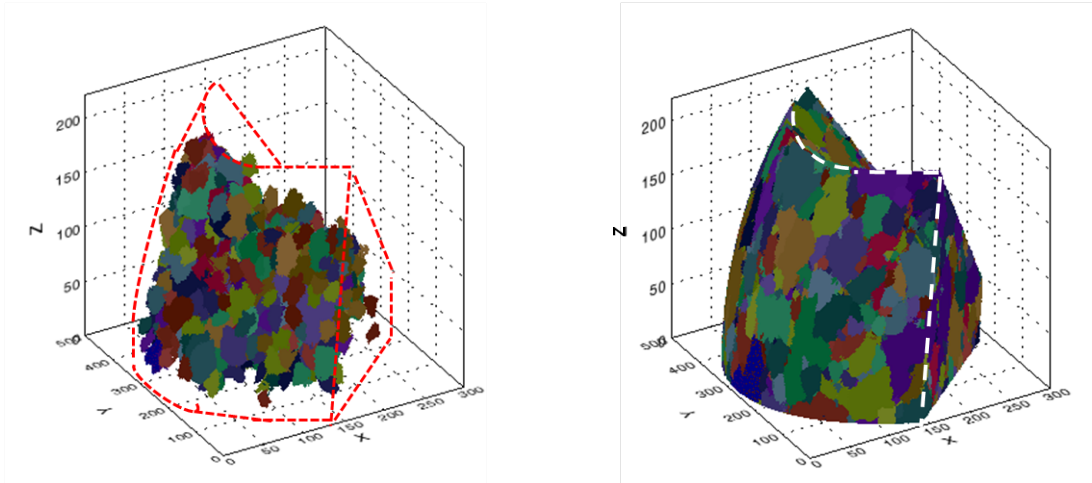


**Figure 2.** The right panel shows the initial Voids in the observational data of SDSS DR7 and the Left panel shows the final voids after the omission of small and edge voids.

**Table 1.** Characteristics of our volume-limited samples.

	Observation	Simulation
Sample Volume (Mpc/h) <sup>3</sup>	$\approx 1.2 \times 10^7$	$\approx 1.2 \times 10^7$
Number of galaxies	68702	68701
Number of field galaxies	5873	5377
Number of wall galaxies	62829	63324
Number of void galaxies(field + faint)	26859	43666
Mean galaxy separation (Mpc/h)	6.22	6.35

#### 4 THE VOID-FINDER ALGORITHM

Various definitions of voids have been previously suggested (Kirschner et al. 1981; Kauffmann & Fairall 1991; Sahni et al. 1994; Benson et al. 2003) and a number of void-finding algorithms, a number of which presume voids to be nearly spherical, have been developed (see *e.g.* Hoyle & Vogeley (2002)). We have tried to avoid this limitation and have developed a method based on the original algorithm of Aikio & Maehoenen (1998) (Hereafter AM Algorithm). The AM algorithm was originally written in 2D and we have extended it to 3D and adapted it for application to large datasets. The algorithm does not constrain the voids to be of any particular shapes and hence can be used to study the shapes of the voids and their deviations from sphericity.

Prior to the application of AM algorithm to our Volume-limited galaxy sample, we classify galaxies as wall or field galaxies. To distinguish between wall and field galaxies, we introduce the parameter  $d$  which is related to the mean distance of the third nearest neighbour,  $d_3$ , and the standard deviation of its value,  $\sigma$ , by the following expression: ( $d = d_3 + 1.5\sigma$ ) (Hoyle & Vogeley 2002). In our volume-limited galaxy sample, all galaxies with third nearest neighbour distance,  $d_3$ , greater than this selection parameter,  $d$ , are taken to be field galaxies and removed from the galaxy sample and the remaining objects are identified as wall galaxies. We remark that a field galaxy may lie within a void region, hence a void galaxy, whereas wall galaxies all lie in the cosmic filaments and clusters and by definition are not to be found in voids.

We find that the selection parameter,  $d$ , for observation and simulation data are 5.96 and 6.16 Mpc/h respectively which results in 9% of the galaxies in the observation and 8% in the simulation

being identified as field galaxies. The details of the samples are given in Table 1.

To implement the AM algorithm, wall galaxies are gridded up in cells of size 1 Mpc/h. The AM algorithm starts on the Cartesian gridded wall galaxy sample by defining a Distance Field (DF). For a given grid in three dimensional galaxy sample the DF is defined as the distance to the nearest particle. Then according to the value of DF for the closest neighbours of each grid, the local maxima of DF *subvoid* is calculated. In order to assign each element in the grid sample to a subvoid, the "Climbing Algorithm" (Schmidt et al. 2001) is used where for a unit cell bounded by the grid points, *i.e.* an elementary cell, the gradient in DF to each of the neighbouring cell is calculated. In this method, the elementary cell and every other cell along the climbing route is then assigned to a subvoid. Finally if the distance between two subvoids is less than both DFs then they will be joined together into a larger void.

The *void volume* is estimated using the number of grid points inside a given void multiplied by the volume associated with the grid cell. For each void, we define its *effective radius* ( $r_{\text{eff}}$ ) as the radius of a sphere whose volume is equal to that of the void.

The configuration of each void in this algorithm depends on the grid points and subsequently we determine the *void centre* as the centre of mass identified by the positions of the grid points that enclose an elementary cell. Following this standard method and giving the same weight to all elementary cells, the centre of each void can be written as

$$X_V^j = 1/N \sum_{i=1}^N x_i^j \quad (1)$$

where  $x_i^j$  ( $j = 1, 2, 3$ ) are the locations of elementary cells and  $N$  is the number of cells in the void  $V$ . The *shape of a voids* is then characterized by the ratio of the total number of grid points, which lie between its centre and its effective radius, to its volume. This ratio is an indicator of the deviation of the shape of the void from sphericity. Ideally, for a spherical void this ratio is equal to one.

In the next section, we apply this algorithm to the SDSS DR7 and the mock catalog to construct catalogues of voids and to study their characteristics.

**Table 2.** Statistics of void in the observation of SDSS DR7 and mock simulated catalogues

	Observation		Simulation	
	Number	Volume (Mpc/h) <sup>3</sup>	Number	Volume (Mpc/h) <sup>3</sup>
All Voids	4616	12541454	4847	12555147
Edge Voids	1148	7844214 (62.5%)	1193	7646672 (61%)
Small Voids ( $r_{eff} < 7\text{Mpc/h}$ )	3001	722062 (5.8%)	3085	845753 (6.7%)
Voids in the final sample	467	3975178 (31.7%)	569	4062722 (32.3%)

**Table 3.** The sizes and sphericities of voids in the observation and simulated mock catalogues

	Effective Radius (Mpc/h)			Max-length (Mpc/h)			Surface (Mpc/h) <sup>2</sup>			Sphericity		
	Max	Min	Median	Max	Min	Median	Max	Min	Median	Max	Min	Median
Observation	30.47	7.02	9.65	108.6	19.9	32.3	35414	1214	2588	0.82	0.22	0.71
Simulaion	28.15	7.00	9.08	103.1	19.1	30.1	33018	1210	2276	0.84	0.12	0.72

## 5 VOIDS IN THE SDSS DR7 REDSHIFT SURVEY AND IN THE MOCK CATALOG

We have identified 4616 and 4847 voids of different sizes and shapes in the SDSS DR7 survey and in the mock catalog respectively. We have avoided problems due to boundary effects, by selecting voids that lie completely inside geometrical boundaries of our catalogues. Therefore, *Edge voids*, those that touch the survey boundaries, are removed from our void catalog due to their under-estimated volumes and distorted shapes (see Fig.2).

The size of each void is characterized by its effective-radius, defined in the previous section. To avoid counting spurious voids, we set a threshold of 7 Mpc/h for the minimum size of effective radii of voids in both samples. This threshold is larger than mean distance between galaxies in the sample and helps to eliminate seemingly *Small Voids* from the sample. After removing all of the spurious voids, we end up with about 467 and 569 voids, in our volume-limited sample of SDSS DR7 survey and mock simulation data respectively which occupy  $\sim 32\%$  of the volumes of the samples. In Table.2, the statistics of voids are given. Hereafter all of the analysis are carried out on voids in the final sample, obtained after the elimination of small and edge voids.

Table 3 compares the statistical properties of voids in the observed and mock catalogues. It shows that the median of void sphericity in both samples are nearly  $\sim 0.70$  which indicates that voids tend to be mostly spherical. Fig. 3 also shows that voids tend to become more spherical with increasing radii. There is a good agreement between the mock catalog and the SDSS observation although the observed voids seem to be marginally more spherical in general. More and better data is needed to see if the marginal difference reported here is of any significance.

## 6 ABUNDANCE OF LARGE VOIDS: THE SDSS DR7 OBSERVATION VERSUS THE MOCK CATALOG

We have compared the distribution of the sizes of voids in the observation against the simulated mock catalogues. Fig. 4 shows that the volume occupied by voids is larger in the simulation than in the observation. In particular, both the histograms and the cumulative plots show that the largest voids are absent from the simulation whereas they are present in the observation.

The problem of large voids could be related to the over-abundance of small galaxies which would subsequently divide large

voids into smaller ones. However, this could be resolved by proper biasing in modeling of galaxy formation and evolution. Hence, the problem of large voids could be due to the shortcoming of the semi-analytic model of galaxy formation for the mock catalog that we have used here. A recent study that also compared the SDSS DR7 voids with those taken from a SPH simulation and a halo-occupation model and hence uses a different model of galaxy evolution, seems to indicate that the distribution of the sizes of voids agree in the two samples (Pan et al. 2012). Hence, such void properties could be of potential importance in distinguishing between different galaxy formation scenarios.

## 7 OBSERVED SDSS VOIDS ARE LESS LUMINOUS THAN THOSE IN THE MOCK CATALOG

Prior to comparing the luminosities of the voids between simulation and observation, we need make sure that there is no bias between the two samples. In Fig. 5, we have plotted the histogram of the absolute magnitudes of field and faint galaxies that are found in the voids in the two catalogues. The figure shows that although the number of void galaxies in mock catalog is larger than that in the observation, the distributions are the same in both catalogues. Min and Max magnitudes are nearly the same, namely  $M \sim -16.5$  in the and  $M \sim -22$  in the observation and the simulation. This demonstrates that there is no bias between the two samples.

We comment that the void galaxies could be field galaxies or be field and faint galaxies. We recall that the field galaxies are in the luminosity ranges  $M < -19.9$  in the observation and  $M < -20.16$  in the simulation, but faint galaxies are less luminous than these threshold set in our volume-limited sample (see Fig.5).

We have compared both the total luminosity of the voids and their luminosity per unit volume between the observation and the simulation. The comparisons are shown in Fig. 6. The lower panel of Fig. 6 shows that If we consider faint and field galaxies, large voids are clearly more luminous in the mock catalog than in the observation. However, the top panel of Fig. 6 shows that if we consider only field galaxies, then this discrepancy becomes less prominent. We emphasize that the minimum magnitude cut-off for both samples is nearly the same when faint galaxies are considered (see Fig.5). This discrepancy could be a sign of the over-abundance of small faint galaxies in the simulation. The problem of empty voids could be related to the lack of large power of  $\Lambda\text{CDM}$ , in spite of the fact that the value of  $\sigma_8$  used here is 0.9 which is larger than its

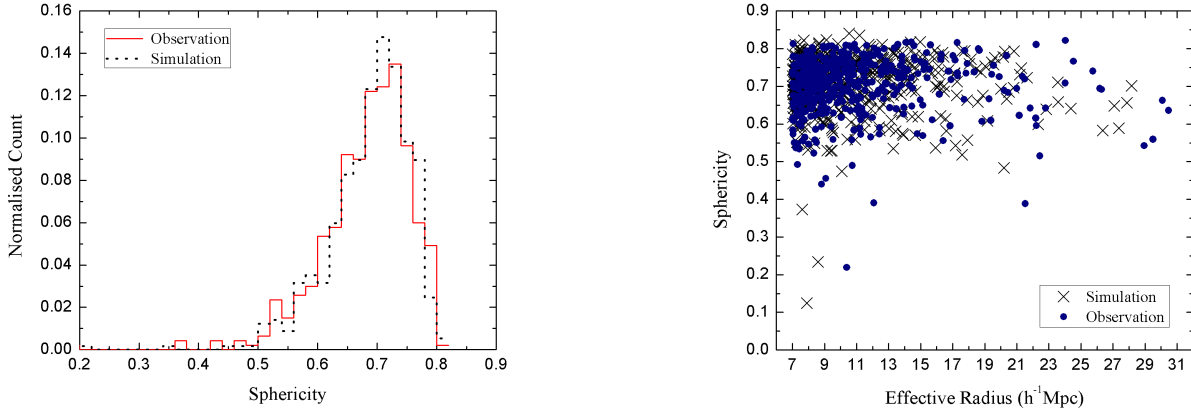


**Figure 3.** Left panel shows the distribution of sphericity is skewed towards larger sphericities, *i.e.* voids are mostly spherical. The right panel shows a plot of the sphericities versus the equivalent radii of the voids demonstrating that voids become more spherical with increasing radii. There is no significant difference between the observation and the simulation and more data would be needed to establish any disagreement between the two.

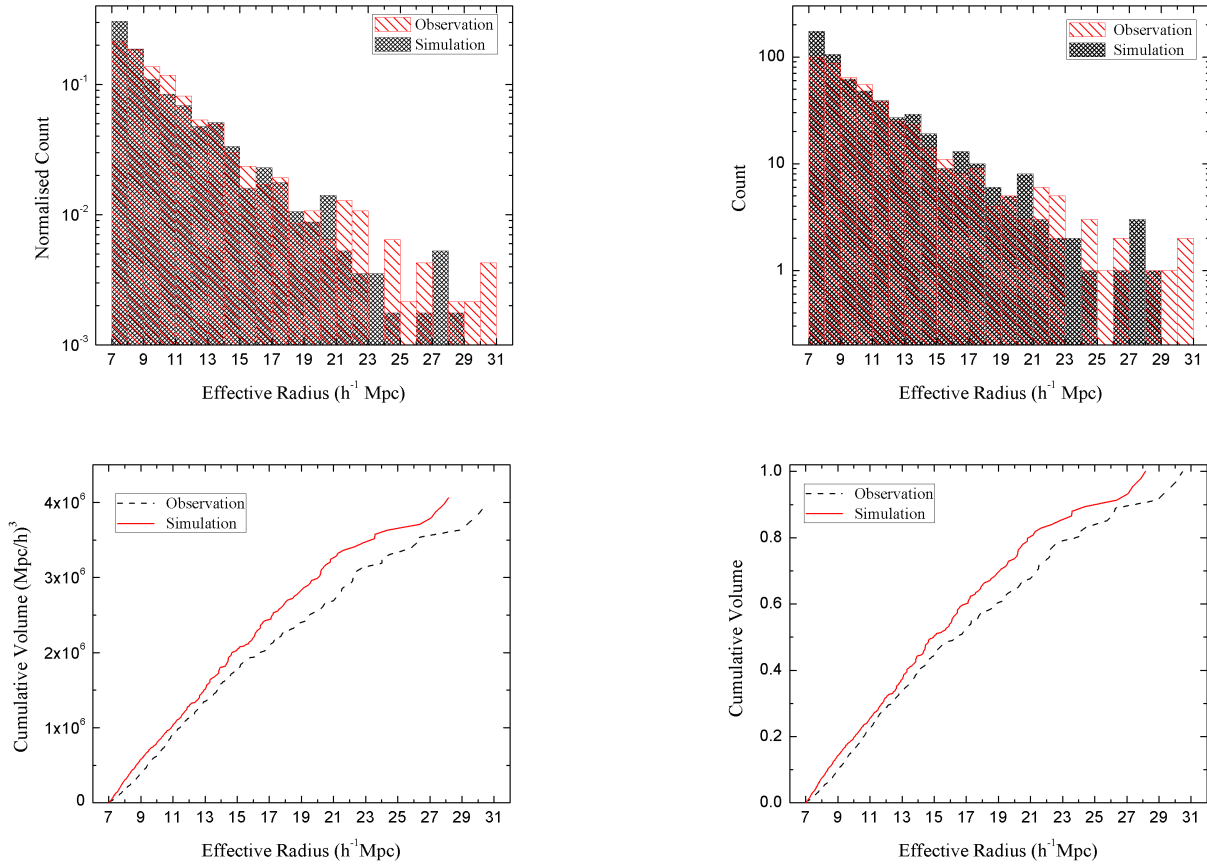


**Figure 4.** Top panel: Distribution of the sizes of voids in the observation and the simulation: larger voids are more abundant in the observation. Bottom panel: Cumulative plots of number of voids against their equivalent radii shows again that larger voids are more abundant in the observation. The bottom plots show the volume/radius cumulative curves where both the cumulative volume and normalize volumes are plotted against the effective radii of the voids. The histograms show that at large radii, there are more voids in the observation than in the simulation. The lower panel demonstrate that the number and volume of voids are, in general, higher in the simulation than in the observation (see Table.2).

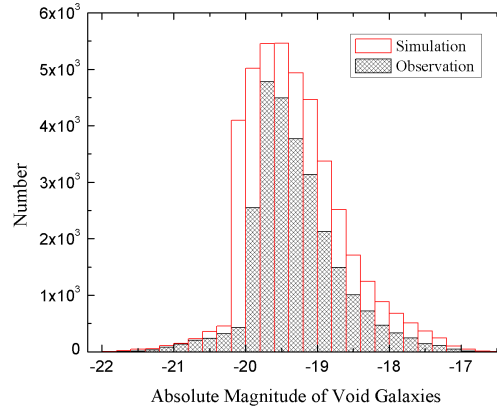


**Figure 5.** Number of void galaxies is plotted against their absolute magnitudes. The range of luminosities of void galaxies are nearly the same for both simulation and observation, hence demonstrating that there is no bias imposed on the calculation of the luminosities of voids. The figure shows that voids in the simulation contain more galaxies, in almost all magnitude bands and hence are more luminous than those in the observation.

present value of 0.8 given by WMAP7. Hence, this discrepancy is expected to be more significant, when using WMAP7 value of  $\sigma_8$ , than found here.

## 8 CONCLUSION

In this paper, we have carried a parallel study of the voids in the SDSS DR7 redshift survey and in a mock catalog. The later is extracted from the Millennium I simulation and aims at replicating observational biases and limitation of the SDSS DR7 catalog.

We have found that the total number and the volume occupied by the voids are larger in the simulation than in the observation. We find 467 voids in SDSS DR7 and 569 in the mock catalog. The voids pseudo-radii or effective radii (*i.e.* radii of an equivalent spherical volume) range from 7 to 31 Mpc/h. The sphericities of voids also have similar distributions in the observation and the simulation. The voids also tend to become more spherical with increasing effective radii. Furthermore, large voids are less abundant in the simulation and the mean luminosities of void, as defined by the sum of the luminosities of the galaxies they contain, are larger in the simulation. The problem of abundance of large voids, could be related to the problem of over-abundance of small haloes in  $\Lambda$ CDM that would then divide large voids into smaller ones in the simulation. However, this problem is usually taken care of in models of galaxy formation by suitable biasing or quenching of galaxy formation on small scales. The persistence of this problem could demonstrate that the semi-analytic model of galaxy formation used in the mock catalog does not suppress galaxy formation in small voids efficiently.

We have also found that voids are in general more luminous in the simulation than in the observation. This could be related to the lack of power of  $\Lambda$ CDM on large scales. The value of  $\sigma_8$  used in the Millennium I simulation has the high value of 0.9 as compared to the value of 0.8 given by the WMAP7. The problem of empty voids could then become even more significant if the current value of  $\sigma_8$  was used in the simulation. Hence, either the ingredients used in the semi-analytic model do not correctly reproduce the observations or on a more fundamental level, the power spectrum of  $\Lambda$ CDM has too much power on small scales and too little on large scales and these cannot be remedied by realistic models of galaxy formation.

**Acknowledgments:** We thank Sepehr Arbabi for collaborations and Habib Khosroshahi, Guilhem Lavaux, Gary Mamon, Joe Silk and David Weinberg for discussions. RM thanks IPM and ST and KV thank IAP for hospitalities.

## REFERENCES

- Abazajian, K. N., Adelman-McCarthy, J. K., Agüeros, M. A., et al. 2009, *ApJS*, 182, 543
- Aikio, J., & Maehoenen, P. 1998, *ApJ*, 497, 534
- Benson, A. J., Hoyle, F., Torres, F., & Vogeley, M. S. 2003, *MNRAS*, 340, 160
- Blaizot J., Wadadekar Y., Guiderdoni B., Colombi S. T., Bertin E., Bouchet, F. R., Devriendt, J. E. G., & Hatton, S. 2005, *MNRAS*, 360, 159
- Blanton, M. R., & Roweis, S. 2007, *AJ*, 133, 734
- Blanton M. R., Lin H., Lupton R. H., Maley F. M., Young N., Zehavi I., Loveday J., 2003a, *AJ*, 125, 2276
- Bothun, G. D., Beers, T. C., Mould, J. R., & Huchra, J. P. 1986, *ApJ*, 308, 510
- Bower R. G., Benson A. J., & Crain, R. A., 2012, *MNRAS*, 422, 2816
- Bower R. G., Benson A. J., Malbon R., Helly J. C., Frenk C. S., Baugh C. M., Cole S., & Lacey C. G., 2006, *MNRAS*, 370, 645
- Colberg, J. M., Pearce, F., Foster, C., et al. 2008, *MNRAS*, 387, 933
- Copi, C. J., Huterer, D., Schwarz, D. J., & Starkman, G. D. 2006, *MNRAS*, 367, 79
- Davis, M., Huchra, J., Latham, D. W., & Tonry, J. 1982, *ApJ*, 253, 423
- da Costa, L. N., Geller, M. J., Pellegrini, P. S., et al. 1994, *ApJL*, 424, L1
- da Costa, L. N., Pellegrini, P. S., Sargent, W. L. W., et al. 1988, *ApJ*, 327, 544
- de Lapparent, V., Geller, M. J., & Huchra, J. P. 1986, *ApJL*, 302, L1
- De Lucia G., Blaizot J., 2007, *MNRAS*, 375, 2
- Efstathiou, G., Ma, Y.-Z., & Hanson, D. 2010, *MNRAS*, 407, 2530
- Efstathiou, G. 2004, *MNRAS*, 348, 885



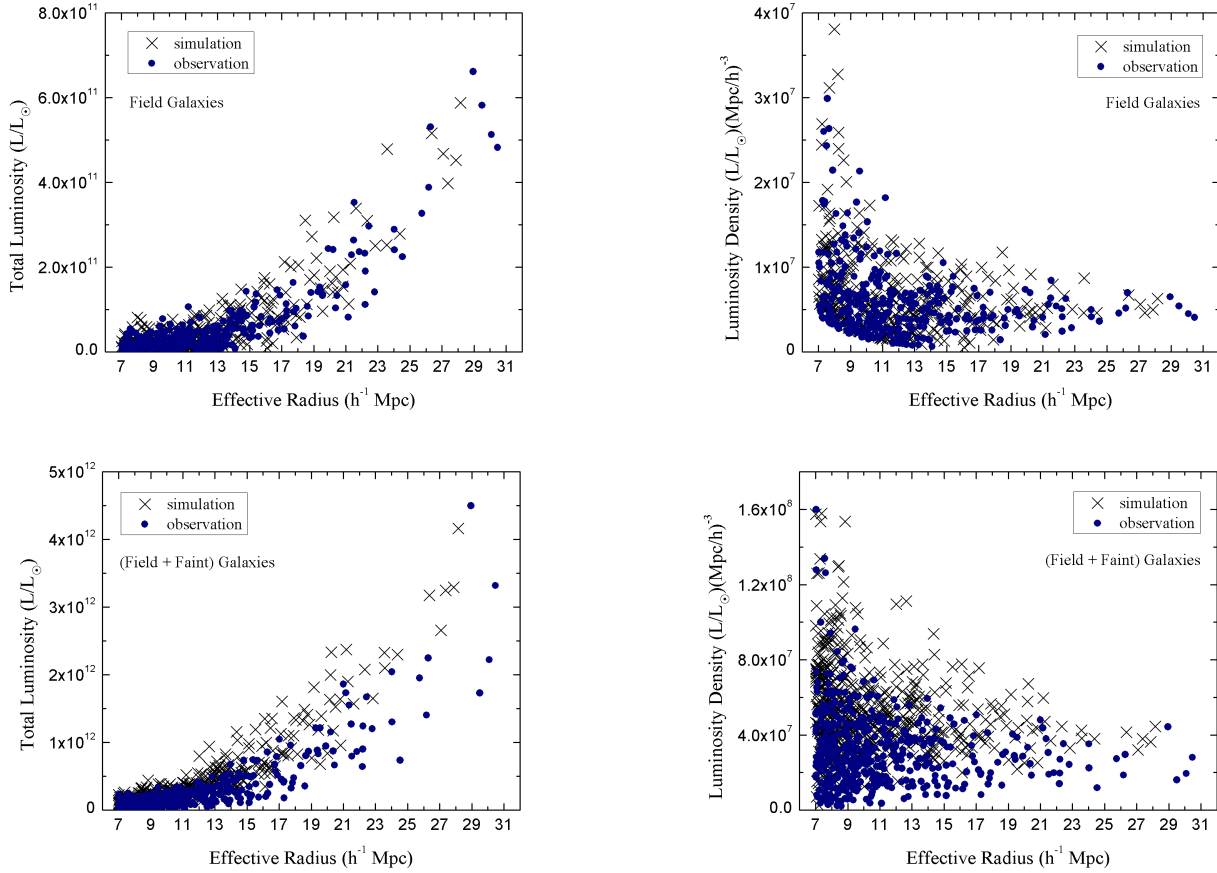


**Figure 6.** *Top panel:* The total luminosity and the luminosity density of field galaxies are plotted against the effective radii of the voids to which they belong. Larger voids are less luminous in the observation than in the simulation. This disagreement becomes more significant when faint objects are also taken into account, as shown in the two plots of the lower panel. Observed voids are clearly less luminous than simulated voids. Note that the luminosity cutoffs are the same for the observation and the simulation when faint galaxies are taken into account. We expect this discrepancy to be even more significant than shown here because our Millennium I simulation uses a larger value of  $\sigma_8$  than given by WMAP7.

Einasto J., Jöeveer M., Saar E., 1980, MNRAS, 193, 353  
 El-Ad, H., & Piran, T. 1997, ApJ, 491, 421  
 Geller, M. J., & Huchra, J. P. 1989, Science, 246, 897  
 Goldberg, D. M., Jones, T. D., Hoyle, F., et al. 2005, ApJ, 621, 643  
 Gottlöber, S., Łokas, E. L., Klypin, A., & Hoffman, Y. 2003, MNRAS, 344, 715  
 Guo Q., White S., Boylan-Kolchin M., De Lucia G., Kauffmann G., Lemson G., Li C., Springel V., Weinmann S., 2011, MNRAS, 413, 101  
 Hoefl, M., Yepes, G., Gottlöber, S., & Springel, V. 2006, MNRAS, 371, 401  
 Hoyle, F., Rojas, R. R., Vogeley, M. S., & Brinkmann, J. 2005, ApJ, 620, 618  
 Hoyle, F., & Vogeley, M. S. 2004, ApJ, 607, 751  
 Hoyle, F., & Vogeley, M. S. 2002, ApJ, 566, 641  
 Kauffmann, G., & Fairall, A. P. 1991, MNRAS, 248, 313  
 Kirshner, R. P., Oemler, A., Jr., Schechter, P. L., & Smetman, S. A. 1981, ApJL, 248, L57  
 Klypin A., Kravtsov A. V., Valenzuela O., Prada F., 1999, ApJ, 522, 82  
 Komatsu E., Smith K. M., Dunkley J., Bennett C. L., Gold B., Hinshaw G., Jarosik N., Larson D., et al. 2011, ApJS, 192, 18

Little, B., & Weinberg, D. H. 1994, MNRAS, 267, 605  
 Menci N., Fiore F., Lamastra A., 2012, MNRAS, 421, 2384M  
 Moore B., Ghigna S., Governato F., Lake G., Guinn T., Stadel J., Tozzi P., 1999, ApJ, 524, 19L  
 Neyrinck, M. C. 2008, MNRAS, 386, 2101  
 Nusser, A., Gubser, S. S., & Peebles, P. J. 2005, PRD, 71, 083505  
 Pan, D. C., Vogeley, M. S., Hoyle, F., Choi, Y.-Y., & Park, C. 2012, MNRAS, 421, 926  
 Patiri, S. G., Prada, F., Holtzman, J., Klypin, A., & Betancort-Rijo, J. 2006, MNRAS, 372, 1710  
 Peebles, P. J. E. 2001, ApJ, 557, 495  
 Platen, E., van de Weygaert, R., & Jones, B. J. T. 2008, MNRAS, 387, 128  
 Plionis, M., & Basilakos, S. 2002, MNRAS, 330, 399  
 Rojas, R. R., Vogeley, M. S., Hoyle, F., & Brinkmann, J. 2004, ApJ, 617, 50  
 Ryden, B. S., & Turner, E. L. 1984, ApJL, 287, L59  
 Sahni, V., Sathyaprakash, B. S., & Shandarin, S. F. 1994, ApJ, 431, 20  
 Schmidt, J. D., Ryden, B. S., & Melott, A. L. 2001, ApJ, 546, 609  
 Shandarin, S., Feldman, H. A., Heitmann, K., & Habib, S. 2006, MNRAS, 367, 1629  
 Shandarin, S. F., & Zeldovich, Y. B. 1989, Reviews of Modern

- Physics, 61, 185
- Springel V. et al., 2005, Nat, 435, 629
- Tikhonov, A. V., & Klypin, A. 2009, MNRAS, 395, 1915
- Tinker, J. L., & Conroy, C. 2009, ApJ, 691, 633
- Tinker, J. L., Conroy, C., Norberg, P., et al. 2008, ApJ, 686, 53
- Tully, R. B., Shaya, E. J., Karachentsev, I. D., et al. 2008, ApJ, 676, 184
- Vogeley, M. S., Geller, M. J., & Huchra, J. P. 1991, ApJ, 382, 44
- Wang, L., Weinmann, S. M. & Neistein, E., 2012, MNRAS, 421, 3450
- Zeldovich, I. B., Einasto, J., & Shandarin, S. F. 1982, Nature, 300, 407